SVN Stroke & Vascular Neurology

STING mediates microglial pyroptosis via interaction with NLRP3 in cerebral ischaemic stroke

Wenyu Li, Nan Shen, Lingqi Kong, Hongmei Huang, Xinyue Wang, Yan Zhang, Guoping Wang, Pengfei Xu, Wei Hu

To cite: Li W, Shen N, Kong L, *et al*. STING mediates microglial pyroptosis via interaction with NLRP3 in cerebral ischaemic stroke. *Stroke & Vascular Neurology* 2024;**9**: e002320. doi:10.1136/svn-2023-002320

► Additional supplemental material is published online only. To view, please visit the journal online (http://dx.doi.org/10.1136/svn-2023-002320).

WL and NS contributed equally.

Received 14 January 2023
Accepted 5 June 2023
Published Online First 3 July 2023

Department of Neurology, The First Affiliated Hospital of USTC, Division of Life Sciences and Medicine, University of Science and Technology of China, Hefei, Anhui, China

Correspondence to
Wei Hu; andinghu@ustc.edu.cn

Pengfei Xu;
xupengfei1026@126.com

ABSTRACT

Background Ischaemia-evoked neuroinflammation is a critical pathogenic event following ischaemic stroke. Gasdermin D (GSDMD)-associated pyroptosis represents a type of inflammation-associated programmed cell death, which can exacerbate neuroinflammatory responses and brain damage. Stimulator of interferon genes (STING) was recently described as a vital innate immune adaptor protein associated with neuroinflammation. Nevertheless, the regulatory effects of STING on microglial pyroptosis post-stroke have not been well elaborated.

Methods STING-knockout and wild-type (WT) mice were subjected to middle cerebral artery occlusion (MCAO). STING small interfering RNA (siRNA) was transfected into BV2 cells before oxygen-glucose deprivation/reoxygenation (OGD/R). STING-overexpressing adeno-associated virus (AAV) and NOD-like receptor family pyrin domain containing 3 (NLRP3) siRNA were administered by stereotaxic injection. 2,3,5-Triphenyl tetrazolium chloride (TTC) staining, TdT-mediated dUTP nick end labeling (TUNEL) staining, Fluoro-Jade C (FJC) staining, neurobehavioural tests, immunohistochemistry, cytokine antibody array assay, transmission electron microscopy, immunoblot, Enzyme-linked immunosorbent assay (ELISA) and quantitative real-time polymerase chain reaction (qRT-PCR) were carried out. Co-immunoprecipitation assays were used to investigate the interplay between STING and NLRP3.

Results STING expression was increased after MCAO and mainly detected on microglia. STING deletion alleviated brain infarction, neuronal damage and neurobehavioural impairment in mice subjected to MCAO. STING knockout suppressed microglial activation and the secretion of inflammatory chemokines, accompanied by mitigation of microglial pyroptosis. Specific upregulation of microglial STING by AAV-F4/80-STING aggravated brain injury and microglial pyroptosis. Mechanistically, co-immunoprecipitation showed that STING bound to NLRP3 in microglia. Supplementation of NLRP3 siRNA reversed AAV-F4/80-STING-induced deterioration of microglial pyroptosis.

Conclusions The current findings indicate that STING modulates NLRP3-mediated microglial pyroptosis following MCAO. STING may serve as a therapeutic target in neuroinflammation induced by cerebral ischaemic/reperfusion (I/R) injury.

WHAT IS ALREADY KNOWN ON THIS TOPIC

⇒ Stimulator of interferon genes (STING) has a central function in pyroptosis-mediated inflammatory response. Additionally, neuroinflammation post-cerebral ischaemia influences the pathogenetic events of ischaemic injury and is associated with lesion progression. However, the mechanism underlying STING-orchestrated inflammation post-ischaemic stroke remains unclear.

WHAT THIS STUDY ADDS

⇒ STING knockout suppressed microglial activation and inflammation via the NOD-like receptor family pyrin domain containing 3 (NLRP3) inflammasome-pyroptosis pathway on brain ischaemia.

⇒ Microglial STING triggered NLRP3 inflammasome activation by interacting with NLRP3.

HOW THIS STUDY MIGHT AFFECT RESEARCH, PRACTICE OR POLICY

⇒ This work may provide new avenues for understanding the correlation between STING and microglial pyroptosis after stroke.

⇒ Targeting of STING signalling can regulate functional recovery in an experimental middle cerebral artery occlusion (MCAO) model, which warrants further clinical development.

INTRODUCTION

Ischaemic stroke represents a major cerebrovascular disease, which results from embolism or thrombosis of a brain artery. Currently applied treatment methods focus on restoring blood flow to reduce neuronal death, but show a narrow time window and do not address post-reperfusion neuroinflammation.[1] The inflammatory response is a prominent hallmark in the pathophysiology of cerebral ischaemia/reperfusion (I/R) injury that is mainly manifested by microglial activation.[2] Moreover, undue and/or prolonged neuroinflammation may cause neuronal damage and neurological impairment following ischaemia brain damage.[3] Pyroptosis, a recently described form of programmed cell death, is triggered by inflammasome induction and is executed by gasdermin D (GSDMD).[4] The N-terminal domain of GSDMD (GSDMD-N) causes plasma membrane perforation, releasing abundant proinflammatory cytokines, which

spread inflammatory signals and exacerbate the inflammatory cascade.[5] GSDMD-mediated pyroptosis in human microglia in vitro and in the ipsilateral cerebral hemisphere of stroke patients has been demonstrated previously.[6 7] These findings suggest that specific interventions to inhibit microglial pyroptosis are potentially valuable.

Stimulator of interferon genes (STING), an important adapter protein involved in DNA-mediated innate immunity, mounts a type I interferon-based response.[8] The STING pathway was reported to be related to inflammatory response and neurobehavioural outcomes in mice with experimental ischaemic stroke.[9] Liao *et al* indicated that cyclic GMP-AMP synthase (cGAS)-STING signalling was involved in microglial histone deacetylase 3-mediating neuroinflammation and cerebral ischaemic injury.[10] Similarly, 25-hydroxycholesterol (25-HC) inhibited middle cerebral artery occlusion (MCAO)-induced neuronal apoptosis by suppressing STING activity.[11] Moreover, a link between STING and pyroptosis was recently revealed. The cGAS-STING pathway orchestrated a lysosomal cell death programme that involved NLRP3 inflammasome activation and pyroptosis in human myeloid cells infected by viruses and bacteria.[12] STING could also trigger lipopolysaccharide (LPS)-induced cardiac pyroptosis by activating NOD-like receptor family pyrin domain containing 3 (NLRP3) in sepsis-induced cardiomyopathy.[13] However, STING's role in cerebral ischaemia and its potential regulatory effects on microglial pyroptosis have not been previously investigated.

Here, using a mouse MCAO model and a BV2 microglia with oxygen-glucose deprivation/reoxygenation (OGD/R) model, this work aimed to elucidate STING's role in ischaemic stroke-induced neuroinflammation and to explore the potential mechanisms involved in NLRP3 inflammasome-mediated microglial pyroptosis.

MATERIALS AND METHODS

Mice

Male C57BL/6J wild-type (WT) mice (20–25 g, 6–8 weeks old) and Sting1-knockout mice (B6/JGpt-*Sting1*^{em10Cd12452}/Gpt, Strain NO. T012747) were purchased from GemPharmatech LLC (Jiangsu, China). The mice were maintained at constant temperature and humidity in specific pathogen-free facility rooms under a 12-hour photoperiod, with food and water at will. The mouse study was carried out as prescribed by the National Institute of Health Guide for the Care and Use of Laboratory Animals (NIH Publications No. 80–23, revised 1996). The study design is shown in online supplemental figure S1. Experimental groups, animal numbers, mortality and exclusion criteria are summarised in online supplemental table 1.

MCAO model establishment, infarct volume and brain oedema measurements and behavioural assays

Mice underwent transient 90-min occlusion of the middle cerebral artery as reported in a previous study.[6] Microglia-specific adeno-associated virus (AAV) was used for STING expression induction in microglia. A small interfering RNA (siRNA) targeting NLRP3 and a STING antagonist (C-176) were used for knockdown experiments. Infarct volume and brain oedema were detected by 2,3,5-triphenyl tetrazolium chloride (TTC) staining. The modified neurological severity score (mNSS), adhesive removal, corner and novel object recognition (NOR) assays were performed for evaluating motor, sensory and cognitive functions. Details on MCAO procedures, TTC staining, behavioural tests and the evaluation of degenerated neurons are provided in online supplemental materials and methods.

Cell culture, OGD/R process and treatment

Murine BV2 microglia were provided by Procell (Wuhan, China). Dulbecco's modified Eagle's medium (DMEM; Gibco, USA) was supplied with 10% fetal bovine serum (Gibco, USA) and 1% penicillin-streptomycin (Gibco, USA) for maintaining cells in a humid environment containing 5% CO_2 at 37°C. OGD/R was carried out as described previously.[14] Typically, the culture medium was substituted with glucose-free DMEM (Gibco, USA), and BV2 cells underwent a 2-hour incubation in humid environment with 5% CO_2 and 95% N_2 at 37°C. Next, cells were subjected to reoxygenation with a normal medium under normoxia for 24 hours in subsequent assays. Cells in the treatment groups were pre-incubated with STING siRNA (si-STING), negative control siRNA (si-NC) or C-176, respectively. The details of experimental procedures are found in online supplemental materials and methods.

Laser speckle imaging, transmission electron microscopy, TdT-mediated dUTP nick end labeling (TUNEL) staining, Fluoro-Jade C (FJC) staining, immunofluorescence, cytokine antibody array assay, Enzyme-linked immunosorbent assay (ELISA), quantitative real-time polymerase chain reaction (qRT-PCR), co-immunoprecipitation and Western blot are described in detail in online supplemental materials and methods.

Statistical analysis

Details on statistical analysis are given in online supplemental materials and methods.

RESULTS

STING expression was dramatically elevated after cerebral I/R injury

To investigate the dynamic changes in STING expression, we performed Western blot to assess penumbral area samples from Sham and MCAO mice at day 1 and 3 post-modelling. The levels of phosphorylated-STING (p-STING) and STING were both continually elevated 1 and 3 days after reperfusion (figure 1A). In addition, p-STING and STING expressions in cultured BV2 cells were increased 12 hours and 24 hours following reoxygenation in comparison with control values (figure 1B). As determined by immunofluorescence, STING was mostly detected in microglia and

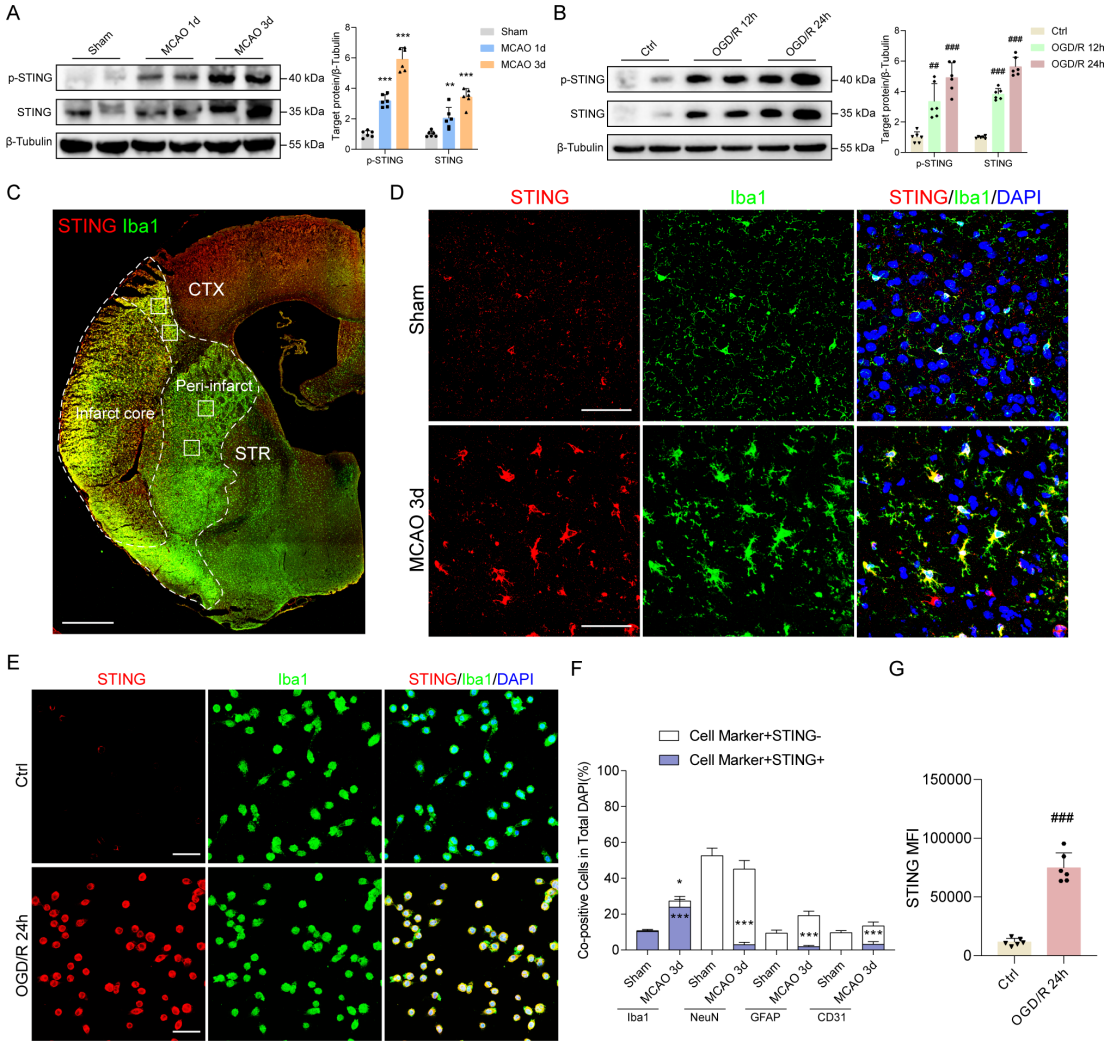

Figure 1 STING expression was upregulated after ischaemic stroke. (A) Immunoblot assessment of p-STING and STING from peri-infarct tissues of mice with experimental MCAO after 1 day or 3 days reperfusion. (B) Protein levels of p-STING and STING in BV2 cells exposed to normal oxygen concentration for 12 and 24 hours after OGD. Data analysis used one-way ANOVA with post hoc Tukey's test. (C) Representative micrograph demonstrating the peri-infarct area delineated by STING and Iba1 staining. Two random high-power fields in the CTX and STR of a given section were examined. Scale bar: 1 mm. (D) Representative immunohistochemical staining for microglia and STING in ischaemic penumbra tissue samples obtained at day 3 after MCAO. (E) Immunofluorescence of STING in cultured BV2 cells following OGD/R. Iba1 served as a microglial marker. Green, Iba1; red, STING; blue, DAPI. (F) Quantification of co-stained cells after focal ischaemia. (G) MFI of STING was quantitated with Image J. Scale bar: 50 µm; n=6/group. Student's t-test. Data are mean±SD. *P<0.05, **P<0.01, ***P<0.001 vs WT Sham mice. $^{\#}P$<0.05, $^{\#\#\#}P$<0.001 vs Ctrl microglia. ANOVA, analysis of variance; CTX, cortex; MCAO, middle cerebral artery occlusion; MFI, mean fluorescence intensity; OGD/R, oxygen-glucose deprivation/reoxygenation; STING, stimulator of interferon genes; STR, striatum; WT, wild type.

to a lesser extent in neurons, astrocytes and endothelial cells in ischaemic penumbra of MCAO mouse models in comparison with Sham animals (figure 1D,F and online supplemental figure S2A–C). Similarly, STING immunostaining signals were enhanced after OGD/R in BV2 cells (figure 1E,G). The above findings indicate that STING is upregulated in the ischaemic penumbra and is mainly produced by activated microglial cells.

STING knockout decreased infarct progression, oedema volume and neuronal damage after MCAO

Male WT and STING$^{-/-}$ mice were used to examine STING's effects on stroke. We measured the changes in ischaemic cortical regional cerebral blood flow (rCBF) by laser speckle imaging (online supplemental figure S3A). The obtained rCBF values were similar between WT and STING$^{-/-}$ mice prior to, during or after 15 min, 24 hours or 72 hours of reperfusion after MCAO (online supplemental figure S3B–D). Next, Western blot confirmed STING was completely knocked out at the protein level in STING$^{-/-}$ mice (figure 2A,B). We selected day 3 as the detection timepoint after ischaemic attack due to the marked increase in STING expression on day 3 after reperfusion. As depicted in figure 2C, infarct volume was overtly reduced from 25.42%±3.25% to 16.37%±2.58% by

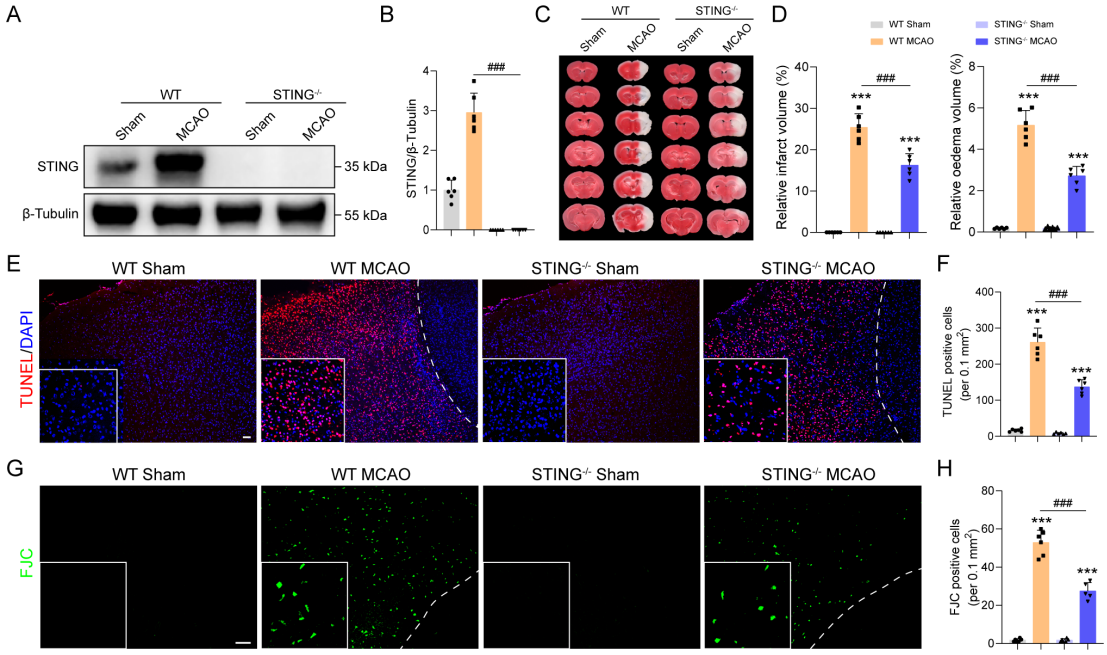

Figure 2 STING suppression ameliorated brain infarction and neuronal damage following MCAO. (A,B) Immunoblot assessment of STING and quantitation. (C) Representative micrographs depicting TTC staining in various groups poststroke. (D) Quantitative assessment of brain infarct and oedema volume. (E–H) The densities of TUNEL-positive and FJC-positive cells were elevated in WT mice following I/R injury, while STING$^{-/-}$ reduced these positive signals in the peri-infarct region. Insets showed images with elevated magnification. Scale bar: 100 µm; n=6/group. Data analysis used one-way ANOVA with post hoc Tukey's test. Data are mean±SD. ***P<0.001 vs Sham mice. ###P<0.001 vs WT MCAO mice. ANOVA, analysis of variance; FJC, Fluoro-Jade C; MCAO, middle cerebral artery occlusion; STING, stimulator of interferon genes; TTC, 2,3,5-triphenyl tetrazolium chloride; TUNEL, TdT-mediated dUTP nick end labeling; WT, wild type.

STING gene knockout following MCAO (figure 2C,D). Likewise, brain oedema volume in STING$^{-/-}$ MCAO mice was decreased to 2.72%±0.45% compared with those of WT MCAO mice (figure 2D). We further perform TUNEL and FJC staining to assess whether STING deficiency could influence post-stroke neuronal damage (figure 2E,G). TUNEL^{+} cells were significantly decreased in the ischaemic cortex of STING$^{-/-}$ MCAO mice versus the WT MCAO mice (figure 2F). Meanwhile, FJC staining showed STING knockout robustly reduced the number of degenerating neurons post-ischaemic stroke versus the WT group (figure 2H).

STING deficiency ameliorated post-stroke long-term neurobehavioural function

Next, we examined the effects of STING on functional outcomes after cerebral I/R injury. The mNSS test showed MCAO decreased sensorimotor function at 1–21 days after surgery, and this effect was partly reserved by STING knockout, with score remission at 3 days post-insult (figure 3A). Similar results were obtained with the adhesive removal and corner tests assessing the sensorimotor function of MCAO mice. STING$^{-/-}$ mice had shorter removal times at 3 days and fewer right turns at 7 days following reperfusion in comparison with control animals (figure 3B,C). Then, the NOR test was carried out to assess cognitive function 21 days post-stroke. STING deficiency significantly alleviated impairments in recognition memory, as indicated by prominently increased recognition index in comparison with WT mice following ischaemic stroke (figure 3D,E).

To explore potential mechanisms underlying relieved long-term neurobehavioural dysfunction in mice with STING$^{-/-}$ deletion, we next detected neuronal degeneration in WT and STING$^{-/-}$ mice 21 days after MCAO. FJC staining microscopic images were acquired from the peri-infarct cerebral cortex (CTX), hippocampal CA1, CA3 and DG regions (figure 3F). In comparison with WT controls, significantly decreased densities were found for FJC-positive neurons in the above areas on STING knockout (figure 3F,G).

STING knockout suppressed microglial and inflammatory activation in the penumbral area of the ischaemic brain

Because microglia are key immune cells and STING has a crucial function in innate immunity,[15] we explored whether STING deficiency affected post-ischaemic inflammatory events. The number and morphological complexity of microglia in cortical and striatal peri-infarct regions were examined. Representative confocal images of all regions, with enlarged single microglia, were shown in figure 4A. According to a morphological assessment of multiple individually delineated microglia, we observed a trend towards a larger microglial soma, increased branch number and decreased average branch length in all analysed regions of MCAO brain samples, while the

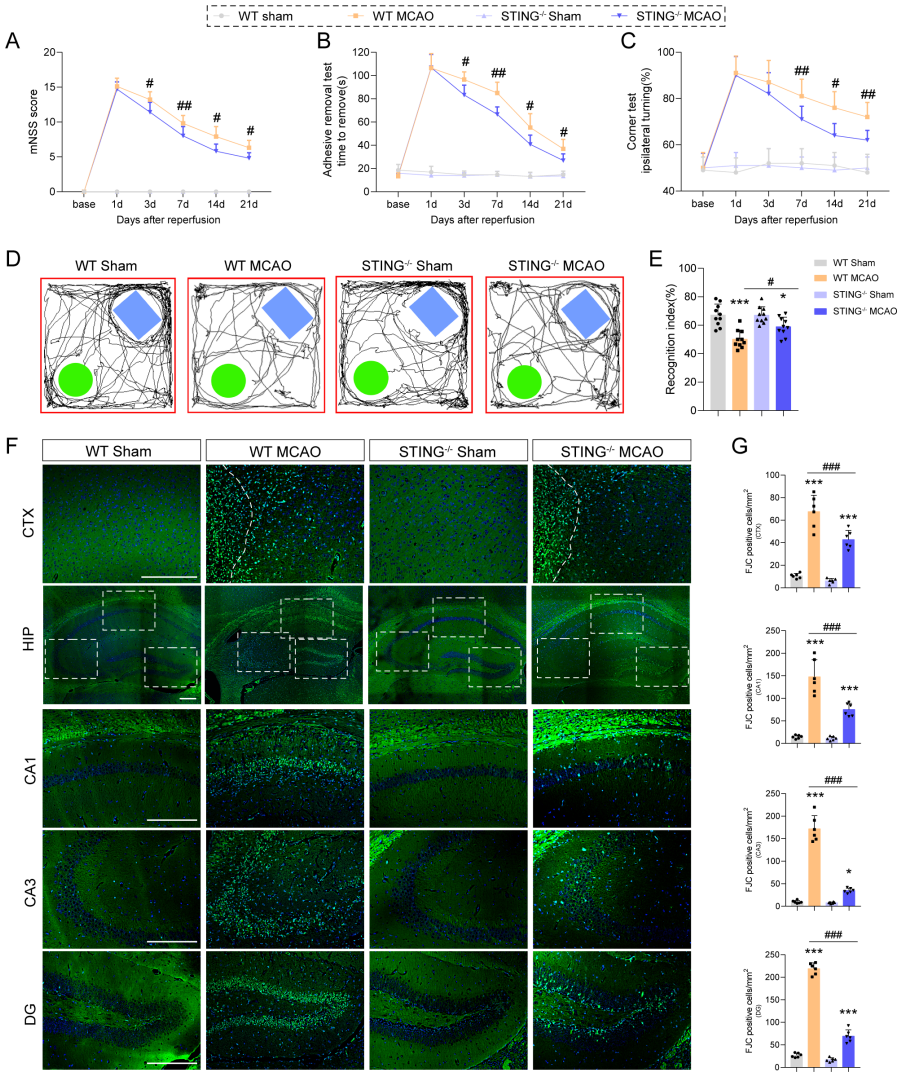

Figure 3 STING deletion improved long-term sensorimotor and cognitive deficits after cerebral ischaemia. (A) mNSS was assessed in male mice before and up to 21 days after injury. (B,C) Sensorimotor impairment was tested by the adhesive removal (B) and corner (C) tests 1–21 days after MCAO. n=10/group. Data analysis used two-way ANOVA with post hoc Tukey's test. Cognitive function was examined by the NOR test on day 21 post-MCAO. (D) Representative tracks. Blue rectangle: novel object. Green circle: familiar object. (E) Recognition index. n=10/group. (F,G) Representative FJC-stained images and quantitation of FJC^+ cells in CTX and hippocampal regions (CA1, CA3, and DG) 21 days after MCAO. Scale bar: 200 µm; n=6/group. Data analysis used one-way ANOVA with post hoc Tukey's test. Data are mean±SD. *P<0.05, ***P<0.001 vs Sham animals. $^{\#}P$<0.05, $^{\#\#}P$<0.01, $^{\#\#\#}P$<0.001 vs WT MCAO group. ANOVA, analysis of variance; CTX, cortex; FJC, Fluoro-Jade C; MCAO, middle cerebral artery occlusion; mNSS, modified neurological severity score; NOR, novel object recognition; STING, stimulator of interferon genes; WT, wild type.

amoeboid morphology of microglia was less typical in MCAO mice after STING deletion (figure 4B). CD68 staining further confirmed reduced numbers of activated microglia in $STING^{-/-}$ mice compared with WT mice after MCAO (figure 4C,D).

Furthermore, we examined the contents of 40 inflammatory cytokines in the penumbral area of the ischaemic brain using an antibody array (figure 4E). Interestingly, genetic deletion of STING decreased the protein levels of 8 proinflammatory cytokines, including C5a, G-CSF, CXCL1, CCL2, CCL12, CCL3, IL-16 and CXCL2 in peri-infarct cerebral areas 3 days post-MCAO (figure 4F).

STING deletion attenuated I/R injury-induced microglial pyroptosis

Given that GSDMD is the effector of pyroptosis,[16] double-labelling of microglia was performed by immunostaining for Iba1 and GSDMD. As depicted in figure 5A, there were more GSDMD-positive microglial cells in the CTX and striatum of the ischaemic penumbra area after MCAO; these trends were reversed by STING deficiency (figure 5A,B). Transmission electron microscopy revealed fewer GSDMD-N formed pores in microglia in the peri-infarct cortical region in the $STING^{-/-}$ MCAO group in comparison with the WT MCAO group (figure 5C). Consistently, GSDMD and GSDMD-N protein amounts,

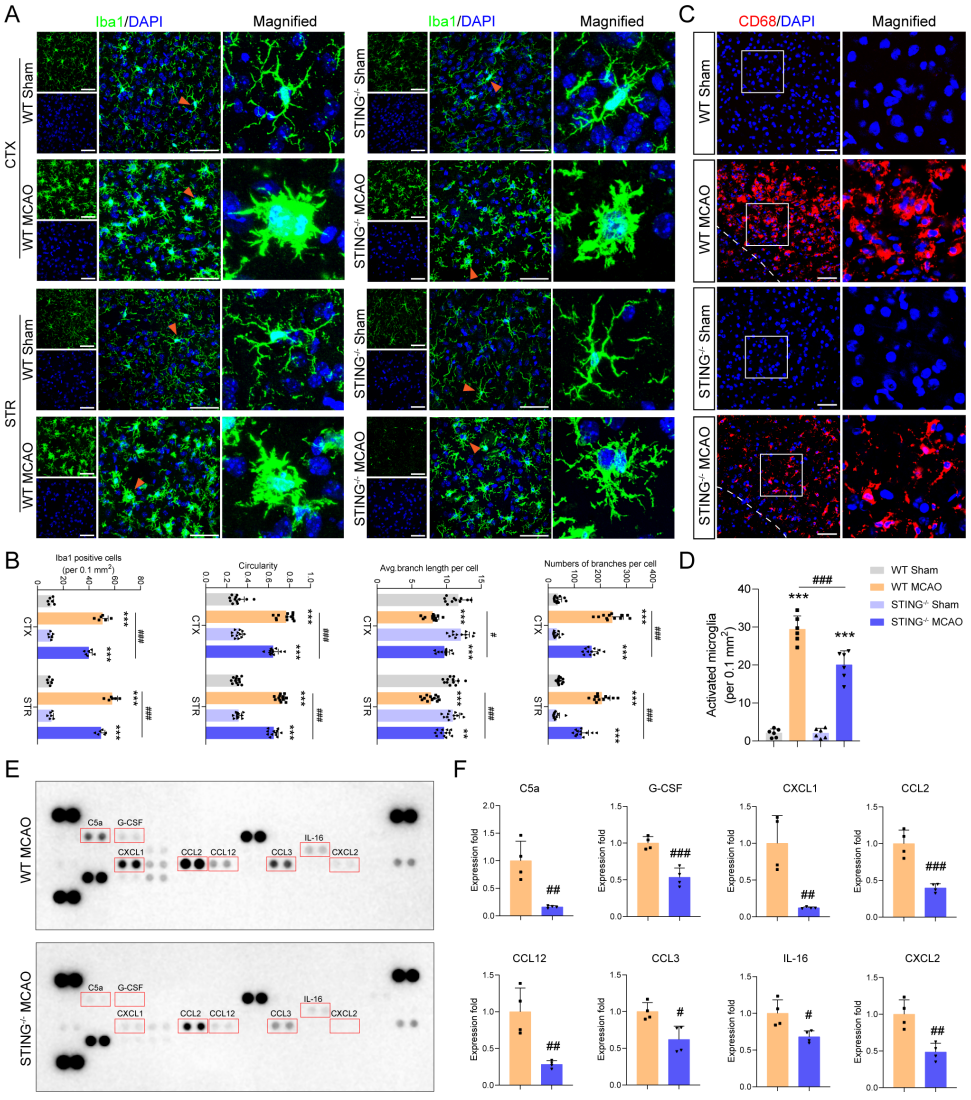

Figure 4 STING promoted post-stroke microglial and inflammatory activation in the peri-infarct area. (A) Altered morphology of microglia in the peri-infarct CTX and STR of WT and STING$^{-/-}$ mice 3 days after MCAO. (B) Quantitation of various parameters (numbers of Iba1-positive cells per 0.1 mm^2, circularity, numbers of branches and average branch lengths) for microglia in each animal. (C,D) Immunostaining and quantification of CD68 in WT and STING$^{-/-}$ mice. Scale bar: 50 µm; n=6/group. Data analysis used one-way ANOVA with post hoc Tukey's test. (E) Representative blots of the cytokine antibody array in experimental groups. (F) Quantitative analysis showed significantly decreased amounts of inflammatory cytokines in the ischaemic brain of STING$^{-/-}$ mice vs WT control mice 3 days after MCAO, including C5a, G-CSF, CXCL1, CCL2, CCL12, CCL3, IL-16 and CXCL2. n=4/group. Student's t-test. Data are mean±SD. $^{**}P<0.01$, $^{***}P<0.001$ vs Sham animals. $^{\#}P<0.05$, $^{\#\#}P<0.01$, $^{\#\#\#}P<0.001$ vs WT MCAO animals. ANOVA, analysis of variance; CTX, cortex; MCAO, middle cerebral artery occlusion; STING, stimulator of interferon genes; STR, striatum; WT, wild type.

as determined by Western blot analysis, were distinctly decreased in STING$^{-/-}$ MCAO mice in comparison with WT MCAO mice (figure 5D). In ELISA, the levels of IL-1β and IL-18 in the ischaemic penumbra were heightened, which were reduced by STING knockout (figure 5E).

To further assess the specific function of STING in microglial pyroptosis in vitro, we used the si-STING to incubate with BV2 cells and performed OGD/R treatment. Transfecting BV2 cells with si-STING significantly downregulated STING determined by Western blot (online supplemental figure S4A,B). Immunofluorescence determined that si-STING treatment resulted in significantly lower mean fluorescence intensity (MFI) values for GSDMD-positive microglia after OGD/R (figure 5F,G). Likewise, the GSDMD and GSDMD-N protein upregulation induced by OGD/R were reversed in si-STING-transfected BV2 microglia (figure 5H,I). Further, ELISA demonstrated that the increased release of IL-1β and IL-18 was reversed by si-STING (figure 5J).

Furthermore, we also used C-176, the pharmacological inhibitor of STING, to examine STING's effects on microglial pyroptosis both in mice and cultured cells (online supplemental figure S5). C-176 reduced the amount of GSDMD$^+$ microglia (online supplemental figure S5A,C,F and G) and GSDMD-N formed pores (online supplemental figure S5B), downregulated the

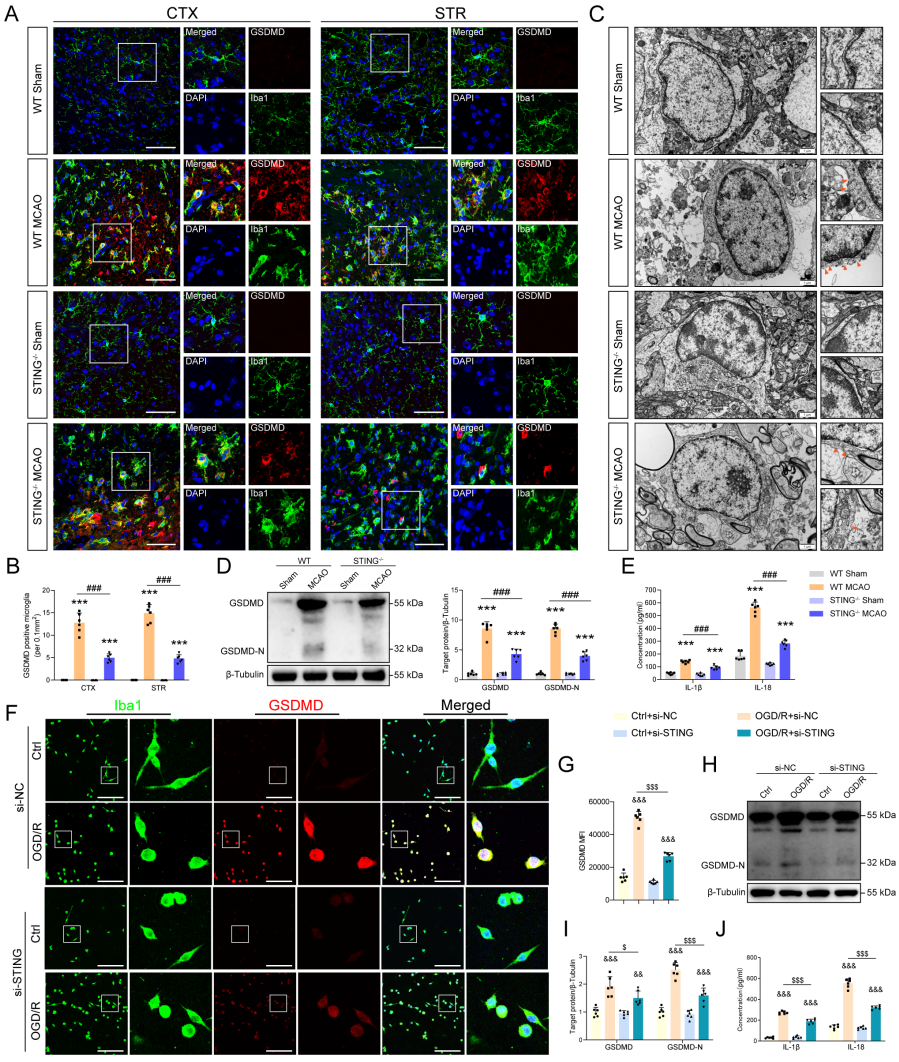

Figure 5 STING knockout alleviated microglial pyroptosis against ischaemic insult. (A,B) Double immunostaining of GSDMD and Iba1 in the CTX and STR of peri-infarct regions and quantitative analysis 3 days following ischaemic insult. (C) Representative transmission electron micrographs of microglial cells in the peri-infarct area. Rightmost panel showed the inset of the left panel at higher magnification. The orange arrows showed pyroptosis pores on the plasma membrane. (D) Immunoblots showing GSDMD and GSDMD-N protein amounts in WT and STING$^{-/-}$ mice with experimental stroke. (E) ELISA analysis of IL-1β and IL-18 levels in brain tissue specimens. (F,G) Immunofluorescence staining of GSDMD and Iba1 in the si-NC and si-STING groups and quantitation of signals; insets depict images at higher magnification. (H,I) Western blot analysis of GSDMD and GSDMD-N in BV2 microglia 24 hours post-reoxygenation. (J) Extracellular releases of IL-1β and IL-18 in OGD/R-induced BV2 microglia. Scale bar: 50 µm; n=6/group. Data analysis used one-way ANOVA with post hoc Tukey's test. Data are mean±SD. $^{***}P<0.001$ vs Sham animals. $^{\#\#\#}P<0.001$ vs WT MCAO animals. $^{\&\&}P<0.01$, $^{\&\&\&}P<0.001$ vs si-NC or si-STING-transfected Ctrl microglia. $^{\$}P<0.05$, $^{\$\$\$}P<0.001$ vs si-NC transfected OGD/R microglia. ANOVA, analysis of variance; CTX, cortex; GSDMD, gasdermin D; GSDMD-N, N-terminal domain of GSDMD; MCAO, middle cerebral artery occlusion; NC, negative control; OGD/R, oxygen-glucose deprivation/reoxygenation; STING, stimulator of interferon genes; STR, striatum; WT, wild type.

expression of GSDMD and GSDMD-N (online supplemental figure S5E,H) and suppressed IL-1β and IL-18 secretion in MCAO mice and OGD/R-exposed BV2 microglia (online supplemental figure S5D,I).

Specific re-expression of microglial STING increased infarct volume and microglial pyroptosis after ischaemic stroke

To examine the relationship between STING and microglial pyroptosis after MCAO, a genetic strategy was used to induce STING expression in microglia. AAV-F4/80-EGFP harbouring a cDNA expression control or STING was stereotaxically administered into the mouse brains 3 weeks prior to MCAO surgery. Under the F4/80 promoter, viruses showing EGFP signals were mostly found in Iba1^{+} microglia in STING$^{-/-}$ MCAO mice (online supplemental figure S6A). Additionally, AAV-STING successfully restored microglial STING levels around the microinjection site, as assessed by Western blot (online supplemental figure S6B). Specific

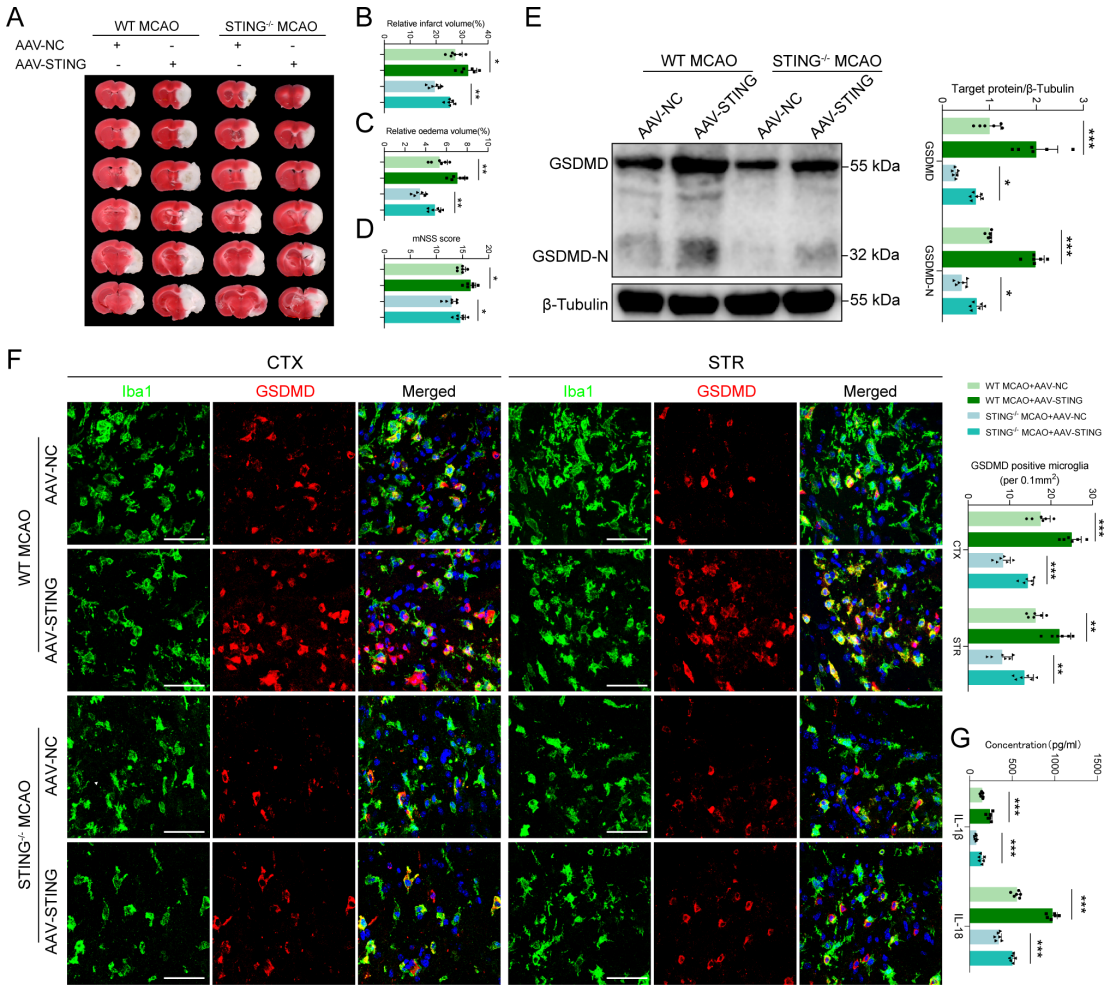

Figure 6 Specific STING upregulation in microglia aggravated infarct volume and microglial pyroptosis after ischaemic stroke. (A) Representative TTC staining indicating ischaemic infarct volume in WT or STING$^{-/-}$ MCAO mice injected with AAV-NC or AAV-STING. (B,C) Quantification of infarct and oedema volume. (D) Quantitation of mNSS scores. Mice in the AAV-STING group had starkly higher scores. (E) Immunoblotting analysis of GSDMD and GSDMD-N in WT or STING$^{-/-}$ MCAO mice receiving AAV, with quantification. (F) Representative images and quantification showing the numbers of GSDMD-positive microglia at the CTX and STR of the peri-lesional tissue. Scale bar: 50 µm. (G) IL-1β and IL-18 production in the ipsilateral CTX were determined with specific ELISA assay kits. n=6/group. Data analysis used one-way ANOVA with post hoc Tukey's test. Data are mean±SD. *P<0.05, **P<0.01, ***P<0.001 vs AAV-NC infected MCAO animals. AAV, adeno-associated virus; ANOVA, analysis of variance; CTX, cortex; GSDMD, gasdermin D; GSDMD-N, N-terminal domain of GSDMD; MCAO, middle cerebral artery occlusion; mNSS, modified neurological severity score; NC, negative control; STING, stimulator of interferon genes; STR, striatum; WT, wild type.

restoration of microglial STING significantly increased brain infarct, oedema volume and mNSS score in WT and STING$^{-/-}$ MCAO mice (figure 6A–D). Compared with the null EGFP reporter virus, AAV-F4/80-STING transfection augmented GSDMD and GSDMD-N protein expressions in the MCAO mice of both genotypes (figure 6E). In a similar fashion, upregulation of microglial STING markedly elevated the number of GSDMD-positive microglia in ischaemic onset (figure 6F) and exacerbated IL-1β and IL-18 secretion (figure 6G).

NLRP3 was required for STING-induced microglial pyroptosis following ischaemic stroke

The STING-NLRP3 pathway is critical for the regulation of glia-associated inflammation.[17] Therefore, we assessed the association between STING and NLRP3 in microglia. Immunostaining showed a co-localization of STING and NLRP3 in Iba1^{+} microglia post-stroke (figure 7A,C). Co-immunoprecipitation further suggested STING interacted with NLRP3 in vivo and in cultured BV2 microglia (figure 7B,D).

We next examined whether STING triggered microglial pyroptosis through the NLRP3 pathway. NLRP3 immunoreactivity showed a marked decrease in Iba1^{+} cells in brain samples from post-ischaemic STING$^{-/-}$ mice compared with WT mice (figure 7E,F). As exhibited in figure 7H, the expression of NLRP3, apoptosis-associated speck-like protein containing a CARD (ASC), cleaved caspase-1, IL-1β and IL-18 were elevated following MCAO, and these

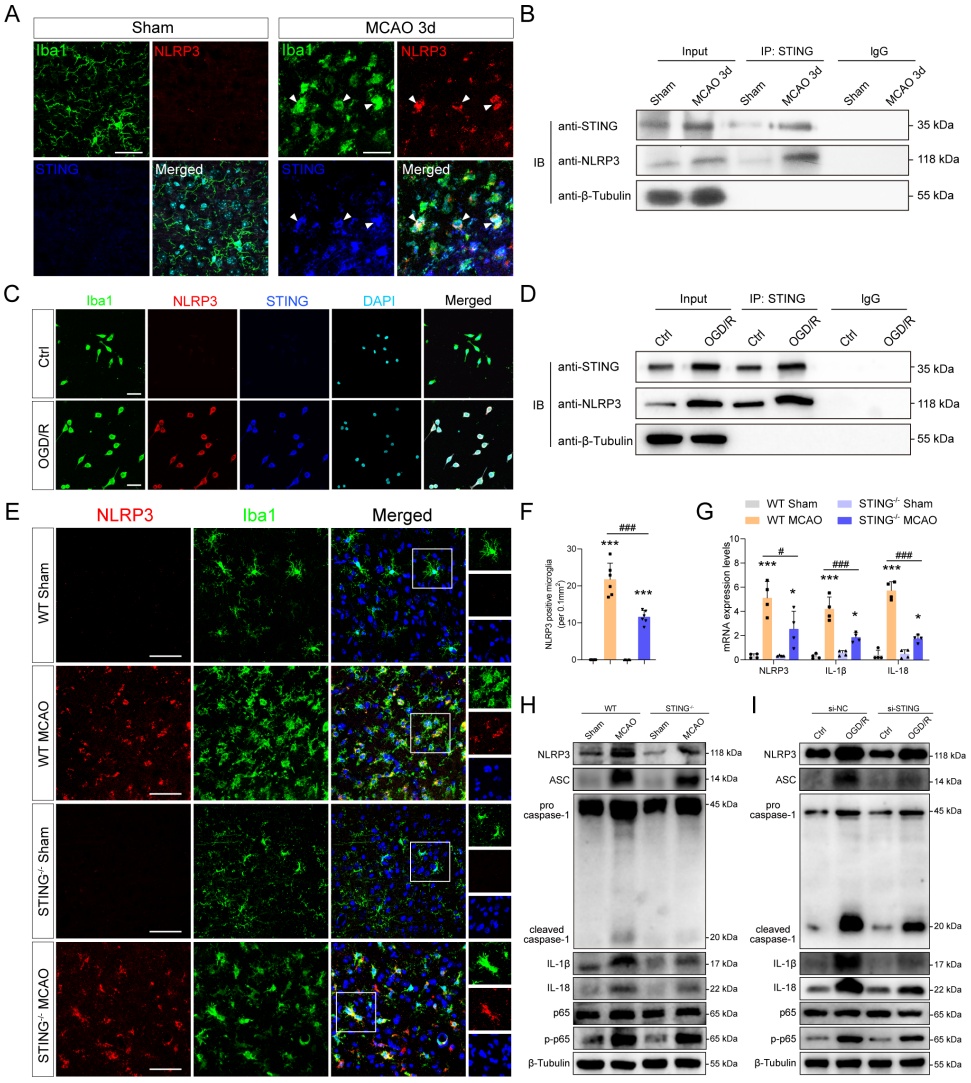

Figure 7 NLRP3 was involved in STING-induced microglial pyroptosis on I/R injury. (A) Immunofluorescent staining of Iba1 (green), NLRP3 (red) and STING (blue) in the ischaemic penumbra of MCAO mice. White arrows indicate a co-localization of STING and NLRP3. (B) Lysates from brain tissues underwent immunoprecipitation with anti-STING antibody. Immunoprecipitates were assessed by immunoblot using antibodies targeting STING and NLRP3. (C) Representative micrographs depicting co-localization of NLRP3 (red) and STING (blue) examined immunohistochemically in microglia (Iba1, green) following OGD/R. (D) Microglia lysates from the control and OGD/R groups underwent immunoprecipitation with anti-STING antibody, followed by Western blot for STING and NLRP3 detection. (E,F) Double immunostaining of NLRP3 and Iba1 in the peri-infarct area and quantitation 72 hours following reperfusion. Insets depict images at higher magnification. (G) NLRP3, IL-1β and IL-18 mRNA levels in WT and STING$^{-/-}$ mice after MCAO or non-injury control procedures. (H) Representative Western blot images and quantitation for NLRP3, ASC, pro-caspase-1, cleaved caspase-1, IL-1β, IL-18, p65 and p-p65 in vivo. (I) Immunoblots showing the protein expression amounts of NLRP3, ASC, pro-caspase-1, cleaved caspase-1, IL-1β, IL-18, p65 and p-p65 in BV2 microglia transfected with si-NC or si-STING. Scale bar: 50 µm. In B, D and G, n=4/group. In A, C, E, F, H and I, n=6/group. Data analysis used one-way ANOVA with post hoc Tukey's test. Data are mean±SD. *P<0.05, ***P<0.001 vs Sham mice. $^{\#}P$<0.05, $^{\#\#\#}P$<0.001 vs WT MCAO mice. ANOVA, analysis of variance; I/R, ischaemic/reperfusion; MCAO, middle cerebral artery occlusion; NC, negative control; OGD/R, oxygen-glucose deprivation/reoxygenation; STING, stimulator of interferon genes; WT, wild type.

effects were apparently reversed by STING knockout (figure 7H and online supplemental figure S7A). We also observed that the level of phosphorylated p65 (p-p65) was increased in the penumbra zone of WT MCAO mice, which was significantly reduced by STING deletion (figure 7H and online supplemental figure S7A). However, the overall level of p65 was not significantly altered (figure 7H and online supplemental figure S7A). Consistently, OGD/R-treated BV2 microglia transfected with si-NC had strengthened the expression of NLRP3, ASC, cleaved caspase-1, IL-1β, IL-18 and p-p65, and the latter effects were reversed in BV2 cells after transfection with si-STING (figure 7I and online supplemental figure S7B). NLRP3, IL-1β and IL-18 mRNA amounts were visibly enhanced in MCAO mice, but were significantly reduced under STING-deficient conditions (figure 7G).

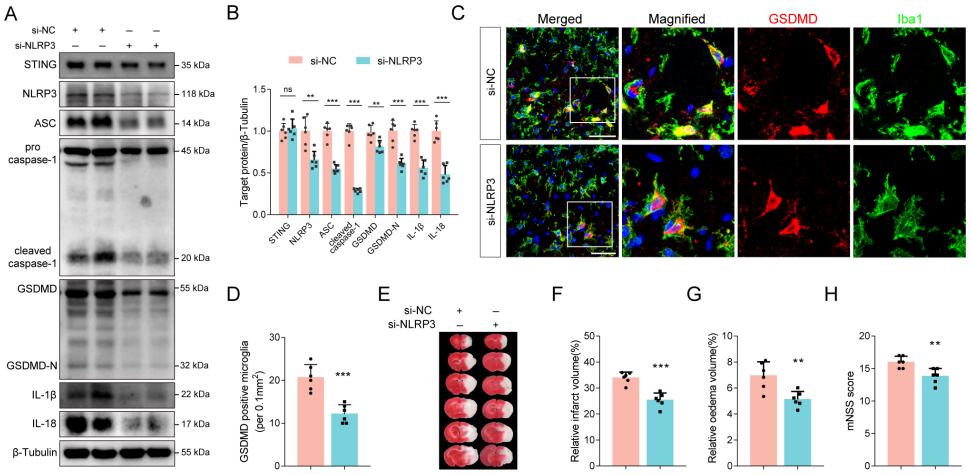

Figure 8 NLRP3 silencing abolished the detrimental effects of STING after MCAO attack. (A) Immunoblot and (B) quantification of STING, NLRP3, ASC, cleaved caspase-1, GSDMD, GSDMD-N, IL-1β, and IL-18 in WT MCAO mice infected with AAV-STING and si-NC or si-NLRP3. (C) Confocal micrographs of MCAO brain samples after double immunofluorescent staining for GSDMD and Iba1. (D) Quantified results for GSDMD expression were shown. (E–G) Representative micrographs depicting TTC staining and quantitation of infarct volume and brain oedema following MCAO. (H) mNSS of AAV-STING and si-NC or si-NLRP3 transfected WT MCAO mice. Scale bar: 50 µm; n=6/group. Student's t-test. Data are mean±SD. ***P*<0.01, ****P*<0.001 vs AAV-STING+si-NC WT MCAO mice. AAV, adeno-associated virus; GSDMD, gasdermin D; GSDMD-N, N-terminal domain of GSDMD; MCAO, middle cerebral artery occlusion; mNSS, modified neurological severity score; NC, negative control; ns, no significant difference; STING, stimulator of interferon genes; TTC, 2,3,5-triphenyl tetrazolium chloride; WT, wild type.

Blocking NLRP3 abrogated the detrimental impacts of STING after ischaemic onset

As NLRP3 is a downstream effector of STING-mediated microglial pyroptosis, whether NLRP3 repression alleviated AAV-F4/80-STING-induced adverse effects after MCAO was examined. Three different siRNA oligonucleotide sequences were constructed to inhibit NLRP3 expression. Of the three siRNAs, si-NLRP3-2 had the most obvious inhibitory effect (online supplemental figure S8A). Besides, double immunostaining demonstrated Cy5-linked si-NLRP3-2 was co-localized with Iba1$^+$ microglia (online supplemental figure S8B). The above findings indicated successful transfection of si-NLRP3-2 into microglia, resulting in reduced NLRP3 expression.

Importantly, si-NLRP3 markedly inhibited NLRP3 expression without affecting microglial STING levels increased by AAV-F4/80-STING transfection after stroke (figure 8A,B). As illustrated in figure 8A, knockdown of NLRP3 significantly reversed STING overexpression-induced increase of GSDMD on microglia, as assessed by immunostaining and immunoblotting (figure 8A–D). In addition, immunoblot also demonstrated the effects of AAV-F4/80-STING on ASC, cleaved caspase-1, IL-1β and IL-18 expressions were countered by si-NLRP3 (figure 8A,B). Silencing of NLRP3 alleviated brain infarction, reduced oedema volume and improved neurological impairment, with decreased mNSS score, in MCAO mice after transfection with AAV-F4/80-STING compared with si-NC treatment (figure 8E–H).

DISCUSSION

This work demonstrated that STING expression was significantly increased and mostly found on microglia in the peri-infarct region following cerebral I/R injury. Genetic deletion of STING improved long-term sensorimotor and cognitive dysfunction in mice subjected to MCAO, which was positively correlated with reduced brain infarction and neuronal damage post-stroke. STING deficiency decreased microglial activation as well as the secretion of pro-inflammatory chemokines. These effects were mediated by STING-induced microglial pyroptosis via the NLRP3 inflammasome pathway (online supplemental figure S9). We also found that STING could bind to NLRP3, which provides a basis for an overt physical interaction between these effectors. After siRNA-mediated genetic inhibition of NLRP3, STING-modulated microglial pyroptosis was reversed, indicating that STING/NLRP3 inflammasome signalling is required for microglial pyroptosis.

The cGAS-STING pathway, including the synthase for the second messenger cGAS and the cyclic GMP-AMP receptor STING, detects pathogens or damaged DNA to induce innate immunity.[18 19] It is known that cGAS activates STING, which regulates many pathophysiological processes in innate immunity.[20] Available evidence confirms that cGAS or STING inhibition obviously attenuates I/R-induced neuroinflammatory pathways and subsequent brain insult. For instance, a cGAS antagonist reduced the expression of pyroptosis-related proteins, decreased neutrophil and microglia numbers and diminished cell death, resulting in infarct volume reduction.[21] siRNA-mediated silencing of cGAS efficiently reduced the secretion of pro-inflammatory molecules during ischaemic stroke to induce microglial M2 polarisation and decrease apoptotic cell death.[22] 25-HC was shown to improve MCAO injury via STING suppression, repressed

autophagy and decreased brain nerve cell apoptosis.[11] A specific antagonist or siRNA was used to alter the function of cGAS or STING in this study. For further investigation of the involvement of cGAS-STING signalling in neuroinflammation, cGAS or STING knockout mice may be applied.

STING is involved in the inflammatory response.[23] Reportedly, cerebral venous sinus thrombosis -mediated inflammation-related disorders were exacerbated by a STING agonist, while such changes were markedly alleviated by STING knockdown with siRNA.[24] STING in macrophages could sense DNA released and activate downstream pro-inflammatory cytokines in a mouse acute pancreatitis model.[25] Besides, STING was activated by the leakage of mitochondrial DNA (mtDNA) to trigger pathological inflammatory response in mice with experimental chronic kidney disease.[26] STING knockdown alleviated neuroinflammation and peripheral pain sensitisation in a rat model of bone cancer pain.[27] Previously, our laboratory demonstrated that STING was mainly expressed on microglia and mediated microglial inflammation by regulating microglial polarisation after cerebral ischaemia.[14] In the present study, genetic knockout of STING in mice was used to further assess STING's effects on the inflammatory response of microglia following ischaemic stroke. We observed that STING deficiency reduced microglial activation as well as the secretion of inflammatory chemokines.

As a form of programmed cell death, pyroptosis has been well documented in different cell types in various diseases.[28] Our previous study revealed that pyroptotic cell death in microglia exacerbated brain damage in an experimental ischaemic stroke model.[6] Increasing evidence demonstrated that STING signalling accelerated pyroptosis-associated damage and inflammasome activation in several pathological conditions.[29] Thus, it is reasonable to hypothesise that STING effectively facilitates microglial pyroptosis in I/R injury. Here, we demonstrated suppressing STING activation by genetic or pharmacological means restrained ischaemia-induced microglial pyroptosis and rescued stroke outcomes.

Indeed, the mechanism by which STING regulates pyroptosis is complex and involves multiple molecular pathways. It was reported that phosphorylated interferon regulatory factor 3 could translocate into the nuclear compartment to mediate STING-driven cardiomyocyte pyroptosis.[13] STING could also induce pyroptosis in tumour cells in the intestinal epithelium via spleen tyrosine kinase (SYK).[30] Moreover, STING-mediated calcium release by the endoplasmic reticulum promotes GSDMD cleavage in sepsis, independent of the NLRP3 inflammasome.[31] The current data revealed that microglial STING could activate pyroptosis via interaction with the NLRP3 inflammasome while activating NF-κB signalling to transcriptionally upregulate NLRP3, IL-1β and IL-18. However, the mechanism underpinning STING-modulated microglial pyroptosis is still not fully elucidated and hence requires further investigation.

The co-immunoprecipitation results suggested STING could bind to NLRP3 and thus lead to NLRP3 activation. However, how STING mediates NLRP3 activation remains poorly understood. Wang and colleagues demonstrated that STING directly interacted with NLRP3 and attenuated the polyubiquitination of NLRP3 to induce NLRP3 activation.[32] According to previous studies, STING activated SYK[30] and SYK-triggered reactive oxygen species (ROS) synthesis to control NLRP3 induction.[33] Other reports also demonstrated that STING regulated a transcriptional programme that controlled ROS production,[34] which was followed by NLRP3 inflammasome activation.[35] These findings suggest STING likely, directly or indirectly, regulates NLRP3 activation.

An unanswered question is what mechanisms underlie STING activation. Previous studies have reported that STING could be activated by cytoplasmic double-stranded DNA (dsDNA)[36] or mtDNA leaked by mitochondrial damage.[37] On the other hand, STING is associated with dsDNA directly, resulting in STING activation.[38] The existence of damaged DNA in microglia was previously reported,[39] providing a basis for STING activation. Furthermore, haemorrhagic shock increased cold-inducible RNA-binding protein levels, which activated STING via the TLR4/MyD88/TRIF pathway to exacerbate inflammation.[40] Nevertheless, other specific mechanisms of STING activation poststroke still warrant further investigation.

This study had certain limitations. First, we evaluated the effects of STING on microglial pyroptosis using global knockout mice and microglial-specific AAV-STING. Although AAV-STING could specifically enhance STING expression in microglia, mice with conditional knockout of STING in microglia are required to validate the current findings. Second, we only used siRNA rather than NLRP3 knockout mice to investigate the contribution of NLRP3 to STING-induced pyroptosis. The effectiveness of local gene knockdown with the siRNA method in the brain has been demonstrated in this and other studies.[41] However, it is currently difficult to use two types of knockout mice for research, so the application of NLRP3 knockout mice may be considered to better confirm this mechanism in future studies.

In summary, we showed that STING was significantly upregulated in microglia in ischaemic stroke, and STING knockout could alleviate ischaemic brain injury and microglial pyroptosis. Furthermore, STING was associated with NLRP3 and activated the NLRP3 inflammasome pathway, thus promoting microglial pyroptosis. These findings reveal STING as a viable molecular target for suppressing microglial pyroptosis and inflammatory response after ischaemic stroke.

Contributors WL and NS performed animal experiments, conducted data analysis and wrote the manuscript. LK and HH performed cell experiments. XW performed behavioural tests. YZ, WG and WH made suggestions to improve the study. PX formulated the study concept, designed the study and modified the manuscript. PX and WH funded this study and supervised the experiments. PX and WH, as

guarantors, were responsible for the overall content. All authors read and agreed to the final manuscript. WL and NS contributed equally to this paper.

Funding This work was supported by the National Natural Science Foundation of China (No. 82101368) and the Anhui Provincial Natural Science Foundation (Nos. 2008085QH368 and 2108085MH272).

Competing interests None declared.

Patient consent for publication Not applicable.

Ethics approval All animal experiments were approved by the Animal Ethics Review Committee of The First Affiliated Hospital of Science and Technology of China (USTC). The animal ethical number: 2023-N(A)-008.

Provenance and peer review Not commissioned; externally peer reviewed.

Data availability statement Data are available on reasonable request. All raw data used in this manuscript are available on reasonable request.

ORCID iD

Wei Hu http://orcid.org/0000-0002-4826-4633

REFERENCES

1 Moussaddy A, Demchuk AM, Hill MD. Thrombolytic therapies for ischemic stroke: triumphs and future challenges. *Neuropharmacology* 2018;134:272–9.
2 Kerr N, Dietrich DW, Bramlett HM, *et al*. Sexually dimorphic microglia and ischemic stroke. *CNS Neurosci Ther* 2019;25:1308–17.
3 Hagberg H, Gressens P, Mallard C. Inflammation during fetal and neonatal life: implications for neurologic and neuropsychiatric disease in children and adults. *Ann Neurol* 2012;71:444–57.
4 Xue Y, Enosi Tuipulotu D, Tan WH, *et al*. Emerging activators and regulators of inflammasomes and pyroptosis. *Trends Immunol* 2019;40:1035–52.
5 Zhang D, Qian J, Zhang P, *et al*. Gasdermin D serves as a key executioner of pyroptosis in experimental cerebral ischemia and reperfusion model both in vivo and in vitro. *J Neurosci Res* 2019;97:645–60.
6 Xu P, Zhang X, Liu Q, *et al*. Microglial TREM-1 receptor mediates neuroinflammatory injury via interaction with SYK in experimental ischemic stroke. *Cell Death Dis* 2019;10:555.
7 Yu F, Huang T, Ran Y, *et al*. New insights into the roles of microglial regulation in brain plasticity-dependent stroke recovery. *Front Cell Neurosci* 2021;15:727899.
8 Zhou J, Ventura CJ, Fang RH, *et al*. Nanodelivery of STING agonists against cancer and infectious diseases. *Mol Aspects Med* 2022;83:101007.
9 Paul BD, Snyder SH, Bohr VA. Signaling by cGAS-STING in neurodegeneration, neuroinflammation, and aging. *Trends Neurosci* 2021;44:83–96.
10 Liao Y, Cheng J, Kong X, *et al*. HDAC3 inhibition ameliorates ischemia/reperfusion-induced brain injury by regulating the microglial cGAS-STING pathway. *Theranostics* 2020;10:9644–62.
11 Lin F, Yao X, Kong C, *et al*. 25-hydroxycholesterol protecting from cerebral ischemia-reperfusion injury through the inhibition of STING activity. *Aging (Albany NY)* 2021;13:20149–63.
12 Gaidt MM, Ebert TS, Chauhan D, *et al*. The DNA inflammasome in human myeloid cells is initiated by a STING-cell death program upstream of NLRP3. *Cell* 2017;171:1110–24.
13 Li N, Zhou H, Wu H, *et al*. STING-IRF3 contributes to lipopolysaccharide-induced cardiac dysfunction, inflammation, apoptosis and pyroptosis by activating NLRP3. *Redox Biol* 2019;24:101215.
14 Kong L, Li W, Chang E, *et al*. mtDNA-STING axis mediates microglial polarization via IRF3/NF-kappaB signaling after ischemic stroke. *Front Immunol* 2022;13:860977.
15 Wang Y-Y, Shen D, Zhao L-J, *et al*. Sting is a critical regulator of spinal cord injury by regulating microglial inflammation via interacting with TBK1 in mice. *Biochem Biophys Res Commun* 2019;517:741–8.
16 Gaidt MM, Hornung V. Pore formation by GSDMD is the effector mechanism of pyroptosis. *EMBO J* 2016;35:2167–9.
17 Zhang L-M, Xin Y, Wu Z-Y, *et al*. STING mediates neuroinflammatory response by activating NLRP3-related pyroptosis in severe traumatic brain injury. *J Neurochem* 2022;162:444–62.
18 Hopfner KP, Hornung V. Molecular mechanisms and cellular functions of cGAS-STING signalling. *Nat Rev Mol Cell Biol* 2020;21:501–21.
19 Zhang W, Li G, Luo R, *et al*. Cytosolic escape of mitochondrial DNA triggers cGAS-STING-NLRP3 axis-dependent nucleus pulposus cell pyroptosis. *Exp Mol Med* 2022;54:129–42.
20 Hu X, Zhang H, Zhang Q, *et al*. Emerging role of STING signalling in CNS injury: inflammation, autophagy, necroptosis, ferroptosis and pyroptosis. *J Neuroinflammation* 2022;19:242.
21 Li Q, Cao Y, Dang C, *et al*. Inhibition of double-strand DNA-sensing cGAS ameliorates brain injury after ischemic stroke. *EMBO Mol Med* 2020;12:e11002.
22 Jiang G-L, Yang X-L, Zhou H-J, *et al*. cGAS knockdown promotes microglial M2 polarization to alleviate neuroinflammation by inhibiting cGAS-STING signaling pathway in cerebral ischemic stroke. *Brain Res Bull* 2021;171:183–95.
23 Sliter DA, Martinez J, Hao L, *et al*. Parkin and PINK1 mitigate STING-induced inflammation. *Nature* 2018;561:258–62.
24 Ding R, Li H, Liu Y, *et al*. Activating cGAS-STING axis contributes to neuroinflammation in CVST mouse model and induces inflammasome activation and microglia pyroptosis. *J Neuroinflammation* 2022;19:137.
25 Zhao Q, Wei Y, Pandol SJ, *et al*. STING signaling promotes inflammation in experimental acute pancreatitis. *Gastroenterology* 2018;154:1822–35.
26 Yan M, Li Y, Luo Q, *et al*. Mitochondrial damage and activation of the cytosolic DNA sensor cGAS-STING pathway lead to cardiac pyroptosis and hypertrophy in diabetic cardiomyopathy mice. *Cell Death Discov* 2022;8:258.
27 Zhang Y, Wang W, Gong Z, *et al*. Activation of the STING pathway induces peripheral sensitization via neuroinflammation in a rat model of bone cancer pain. *Inflamm Res* 2023;72:117–32.
28 Dong Z, Pan K, Pan J, *et al*. The possibility and molecular mechanisms of cell pyroptosis after cerebral ischemia. *Neurosci Bull* 2018;34:1131–6.
29 Sun F, Liu Z, Yang Z, *et al*. The emerging role of STING-dependent signaling on cell death. *Immunol Res* 2019;67:290–6.
30 Gong W, Liu P, Zhao F, *et al*. STING-mediated Syk signaling attenuates tumorigenesis of colitis-associated colorectal cancer through enhancing intestinal epithelium pyroptosis. *Inflamm Bowel Dis* 2022;28:572–85.
31 Zhang H, Zeng L, Xie M, *et al*. TMEM173 drives lethal coagulation in sepsis. *Cell Host Microbe* 2020;27:556–70.
32 Wang W, Hu D, Wu C, *et al*. STING promotes NLRP3 localization in ER and facilitates NLRP3 deubiquitination to activate the inflammasome upon HSV-1 infection. *PLoS Pathog* 2020;16:e1008335.
33 Mócsai A, Ruland J, Tybulewicz VLJ. The SYK tyrosine kinase: a crucial player in diverse biological functions. *Nat Rev Immunol* 2010;10:387–402.
34 Hayman TJ, Baro M, MacNeil T, *et al*. STING enhances cell death through regulation of reactive oxygen species and DNA damage. *Nat Commun* 2021;12:2327.
35 Tschopp J, Schroder K. Nlrp3 Inflammasome activation: the convergence of multiple signalling pathways on ROS production *Nat Rev Immunol* 2010;10:210–5.
36 Chen R, Du J, Zhu H, *et al*. The role of cGAS-STING signalling in liver diseases. *JHEP Rep* 2021;3:100324.
37 Barber GN. STING: infection, inflammation and cancer. *Nat Rev Immunol* 2015;15:760–70.
38 Abe T, Harashima A, Xia T, *et al*. STING recognition of cytoplasmic DNA instigates cellular defense. *Mol Cell* 2013;50:5–15.
39 Matsuda S, Umeda M, Kato H, *et al*. Glial damage after transient focal cerebral ischemia in rats. *J Mol Neurosci* 2009;38:220–6.
40 Chen K, Cagliani J, Aziz M, *et al*. Extracellular CIRP activates STING to exacerbate hemorrhagic shock. *JCI Insight* 2021;6:e143715.
41 Chen S, Peng J, Sherchan P, *et al*. TREM2 activation attenuates neuroinflammation and neuronal apoptosis via Pi3K/AKT pathway after intracerebral hemorrhage in mice. *J Neuroinflammation* 2020;17:168.